High-Resolution ^{1}H NMR Study of the Solution Structure of δ-Hemolysin†

Michael J. Tappin,‡ Annalisa Pastore,‡ Raymond S. Norton,‡,§ John H. Freer,‖ and Iain D. Campbell*,‡
Department of Biochemistry, University of Oxford, South Parks Road, Oxford OX1 3QU, U.K., and Department of Microbiology, University of Glasgow, Anderson College, Glasgow G11 6NU, U.K.
Received July 17, 1987; Revised Manuscript Received October 26, 1987

ABSTRACT: The 26-residue toxin from *Staphylococcus aureus*, δ-hemolysin, is thought to act by traversing the plasma membrane. The structure of this peptide, in methanol solution, has been investigated by using high-resolution NMR in combination with molecular dynamics calculations. The ^{1}H NMR spectrum has been completely assigned, and it is shown that residues 2–20 form a relatively stable helix while the residues at the C-terminal end appear to be more flexible. The structures were calculated only from nuclear Overhauser effect data and standard bond lengths. It is shown that the results are consistent with $^3J_{NH-\alpha CH}$ coupling constants and amide hydrogen exchange rates.

δ-Hemolysin is a small polypeptide of 26 amino acid residues, secreted by *Staphylococcus aureus* (Bernheimer & Rudy, 1986). It has been shown to have lytic effects on membranes of cells and organelles (Yianni et al., 1986). Models that have been proposed for its action include a transmembrane conformation (Freer & Birkbeck, 1982) and the formation of voltage-gated ion channels similar to those proposed for melittin (Tosteson & Tosteson, 1981; Vogel & Jahnig, 1986) and alamethicin (Fox & Richards, 1983). A feature common to these polypeptides is a tendency to form amphiphilic α-helices with one side of the helix more hydrophilic than the other (Eisenberg, 1984). The accommodation of such structures within the lipid bilayer would be consistent with the hydrophobic faces of the helices interacting with the lipid and the formation of a pore involving the hydrophilic faces. If δ-hemolysin forms a helix, then the hydrophilic face will contain an unusually high proportion of charged residues (Freer & Birkbeck, 1982). In total there are four carboxylate groups (three aspartates and the C-terminus) and four lysine amine groups, making it an interesting model for ionic interactions between amphiphilic membrane proteins.

Preliminary X-ray diffraction studies have been carried out on δ-hemolysin crystallized from a solution containing 2-methylpentane-2,4-diol (Thomas et al., 1986). An NMR[1] study on the conformation of δ-hemolysin bound to micelles of deuteriated dodecylphosphocholine has also been published (Lee et al., 1987). We present here a detailed high-resolution proton NMR study of the molecule in methanol solution. The NMR spectrum has been completely assigned, and computer-based techniques have been used to determine the structure.

Materials and Methods

δ-Hemolysin was prepared as previously described (Bhakoo et al., 1982) and further purified on a Waters HPLC system using a 250 mm × 8 mm column packed with Whatman Partisil-10 ODS-3 and methanol as solvent. The absorbance of the eluate was monitored at 280 nm to locate the δ-hemolysin. To obtain maximum recovery, fractions containing impurities were reduced in volume by rotary evaporation and the procedure repeated. After rotary evaporation, the fractions containing δ-hemolysin were dried under nitrogen in a 5-mm NMR tube, dissolved in 0.5 mL of deuteriated methanol, and redried. The samples were then redissolved in 0.5 mL of CD_3OH (MSD Isotopes) or CD_3OD (Fluorochem) to give solutions of 6–7 mM.

^{1}H NMR spectra were recorded on a Bruker AM 500 spectrometer at a temperature of 303 K and referenced to the central component of the quintet due to the CD_2H resonance of methanol at 3.315 ppm. The samples were adjusted to an uncorrected glass electrode reading (pH*) of 3.0.

Double quantum filtered (DQF) COSY (Piantini et al., 1982; Rance et al., 1983) and NOESY (Jeener et al., 1979; Kumar et al., 1980) spectra were recorded by using the TPPI method (Bodenhausen et al., 1980) to produce phase-sensitive spectra and the CYCLOPS phase cycle (Hoult & Richards, 1975) to reduce quadrature errors. A mixing time of 300 ms was used in the NOESY, with a random variation (Macura et al., 1981) of 15 ms. RELAY spectra (Eich et al., 1982) were recorded with τ values of 30 and 60 ms (Bax & Drobny, 1985). Irradiation of the OH resonance was carried out during the relaxation time and, in the case of NOESY, the mixing time. Lower decoupler powers, just sufficient to maintain saturation, were applied during the t_1 periods and the τ delay in the RELAY.

In general, spectra were recorded with a sweep width of 5750 Hz in both dimensions, with 96 scans per t_1 increment in the case of DQF COSY and RELAY and 192 scans per t_1 increment in the case of NOESY. The resulting data matrices (512*4K or 512*2K for the RELAY) were filtered by shifted sine bell multiplication and zero-filled to 2K in t_1 before complex Fourier transformation.

Amide hydrogens that were relatively slow to exchange with solvent were identified by dissolving protonated δ-hemolysin in deuteriated solvent and recording spectra over a period of 24 h.

Molecular dynamics calculations were carried out by using the GROMOS package of programs (Berendsen et al., 1981; van Gunsteren et al., 1983) kindly provided by Prof. W. F. van

† This is a contribution from the Oxford Enzyme Group, which is supported by the SERC. We also thank the MRC and the Wellcome Foundation for financial support.
* Author to whom correspondence should be addressed.
‡ University of Oxford.
§ Permanent address: School of Biochemistry, The University of New South Wales, Kensington, New South Wales, 2033 Australia.
‖ University of Glasgow.

[1] Abbreviations: NMR, nuclear magnetic resonance; DQF COSY, double quantum filtered correlation spectroscopy; NOESY, nuclear Overhauser enhancement spectroscopy; RELAY, relayed coherence transfer spectroscopy; NOE, nuclear Overhauser effect; TPPI, time-proportional phase incrementation; CYCLOPS, cyclic ordered phase scheme; ppm, parts per million; HPLC, high-performance liquid chromatography; RMD, restrained molecular dynamics; EM, energy minimization; rms, root mean square.

0006-2960/88/0427-1643$01.50/0

Gunsteren. Distance geometry based calculations were carried out by using the program DISSMAN. This program, a gift from Dr. W. Braun, is a version of DISMAN (Braun & Go, 1985; Braun et al., 1986) that uses real atoms instead of simplified pseudo-atoms. Although slightly more demanding on computer time, this version allows a more accurate definition of the local geometry. All calculations were carried out on a MicroVax II.

In the DISSMAN and GROMOS calculations, 60 interresidue distances were included as upper bound limits, evaluated by classifying NOESY cross-peak intensities as strong (<0.27 nm), medium (<0.32 nm), and weak (<0.5 nm). The DISSMAN structure determination started with initial conformations generated by using randomly chosen dihedral angles. In addition, two starting structures were created by using an Evans and Sutherland PS300 and the program FRODO. These were an α-helix (HDHL) generated from standard bond angles and a linear extended strand (LDHL).

To reduce the number of van der Waals interaction pairs considered in the restrained molecular dynamics (RMD) runs, interactions were neglected when the atomic separation became greater than 0.8 nm; the list of interactions considered in the calculations was updated every 10 RMD steps of 2 fs. Bond length constraints were applied by using the SHAKE algorithm (Ryckaert et al., 1977; van Gunsteren & Berendsen, 1977). The system was weakly coupled to a thermal bath of T_0 = 293 K with a temperature relaxation time of 0.01 ps during the first 2 ps and 0.1 ps for all the following runs. A force constant of 1000 KJ mol^{-1} Å^{-2} was used for the NMR restraints except in the initial 20 ps. A rather larger force constant of 4000 KJ mol^{-1} Å^{-2} was used for the initial 20 ps for HDHL. In the case of LDHL, convergence was accelerated by using classical dynamics (at constant energy) for a period of 20 ps.

RESULTS

A prerequisite for the determination of protein structure by NMR is assignment of the resonances in the NMR spectrum to specific protons in the molecule. DQF COSY (Rance et al., 1983) and RELAY (Eich et al., 1982) spectra were used to identify the amino acid residue spin systems in δ-hemolysin. In this way, it was possible to identify the complete spin systems of all 26 residues, with the exception of the lysine side chains beyond the β protons. A sequence-specific assignment of spin systems relies on observation of a series of interresidue NOEs, of which the most important are NH_i–NH_{i+1} and α_i–NH_{i+1} (Wüthrich et al., 1982). Using the NOESY spectrum, it was possible to trace a connectivity between sequential NHs along the backbone from the *N*-formyl proton to Asp-4 NH and then from Ile-6 NH to Val-20 NH. The connectivity was lost between Asp-4 and Ile-6, as Asp-4, Ile-5, and Ile-6 have nearly identical NH chemical shifts. An NOE was not observed between Lys-25 NH and Lys-26 NH for similar reasons, while that between Val-20 and Asn-21 was very weak.

A complete sequence-specific assignment of resonances was achieved, as detailed in Table I and illustrated in Figure 1, which shows the NH–αCH cross-peaks in the DQF COSY spectrum.

Figure 2 summarizes the interresidue NOEs observed in δ-hemolysin. It can be seen that, in addition to the NH_i–NH_{i+1} NOEs extending along a large fraction of the molecule, there are a considerable number of α_i–NH_{i+3} and α_i–β_{i+3} NOEs, which are characteristic of a helical structure (Wüthrich et al., 1984).

It was also possible to increase the information content of the NOEs by stereospecific assignment of the methyl groups

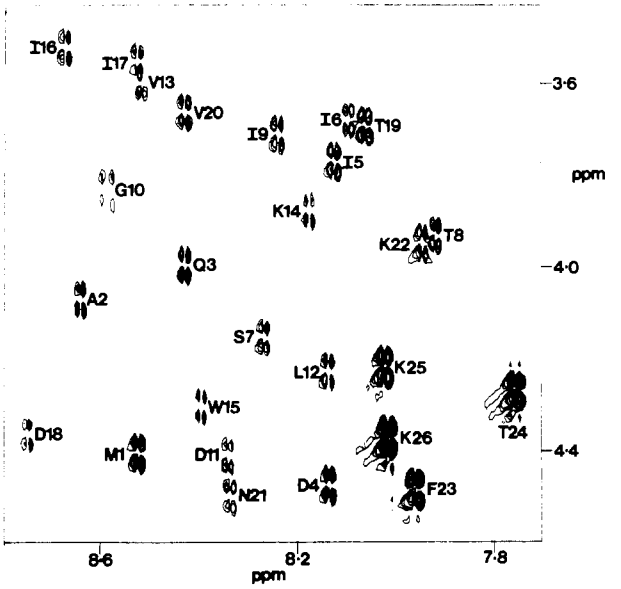

FIGURE 1: 500-MHz phase-sensitive DQF COSY spectrum of δ-hemolysin in CD_3OH (T = 303 K, pH 3.0). The region shown is that containing the NH–αCH cross-peaks, the assignment of which is indicated.

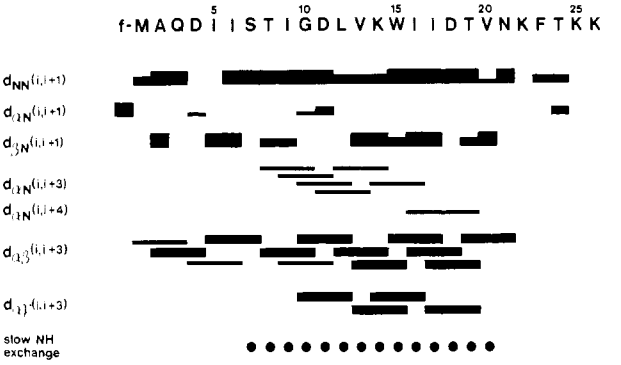

FIGURE 2: Summary of interresidue NOEs observed for δ-hemolysin and used in calculation of the structure. The bar height is an indication of the intensity of the NOE. The amide hydrogens that remained protonated after 12 h in perdeuteriated solvent are also indicated.

of the two valine residues. In both cases large (10 Hz) CHα–CHβ coupling constants were observed together with only one large NH–γCH_3 NOE. This indicates that the side chains adopt the conformation with Hα and Hβ trans. Stereospecific assignment of the methyl groups (Zuiderweg et al., 1985) is thus possible.

Most of the $^3J_{NH-\alpha CH}$ coupling constants were measured from 1D spectra. Where this was not possible, coupling constants were estimated from DQF COSY spectra. The observed values of J are given in the first column of Table II. It can be seen that most of these are less than 6 Hz, which is consistent with the existence of a helical structure for most of the molecule (Pardi et al., 1984).

Structures were calculated from the NMR data by using computer programs based on two fundamentally different approaches, distance geometry (Kuntz et al., 1976) and molecular dynamics (McCammon et al., 1977; Aqvist et al., 1985; Clore et al., 1987).

These structures were calculated by using DISSMAN, a distance geometry based program that operates in dihedral angle space and uses the variable target function method (Braun & Go, 1985). All three structures (labeled DIS1, DIS2, and DIS3), which were calculated as described under Materials and Methods, had a helical region between residues 2 and 19, a small restraints energy, and high potential energy. These

Table I: Assignments of Resonances to Protons in δ-Hemolysin

	NH	αCH	βCH	others	
N-formyl				HCO	8.192
M1	8.524	4.404	2.135	γCH_2	2.610
			2.059		2.550
				ϵCH_3	2.121
A2	8.640	4.073	1.424		
Q3	8.427	4.000	2.126	γCH_2	2.405
					2.325
D4	8.135	4.482	3.035		
			2.883		
I5	8.124	3.770	2.025	γCH_2	1.767
					1.183
				γCH_3	0.915
				δCH_3	0.875
I6	8.096	3.686	1.952	γCH_2	1.711
					1.233
				γCH_3	0.936
				δCH_3	0.841
S7	8.270	4.151	4.022		
			3.877		
T8	7.922	3.933	4.377	γCH_3	1.211
I9	8.242	3.714	1.991	γCH_2	1.812
					1.172
				γCH_3	0.920
				δCH_3	0.819
G10	8.584	3.843			
		3.719			
D11	8.343	4.410	3.158		
			2.715		
L12	8.135	4.230	1.913	γCH	1.857
			1.845	δCH_3	0.959
					0.903
V13	8.517	3.596	2.289	γCH_3 (*pro-S*)	0.964
				γCH_3 (*pro-R*)	1.110
K14	8.174	3.876	2.130		
			1.986		
W15	8.393	4.303	3.590	C(2)H	7.109
			3.400	C(4)H	7.512
				C(5)H	6.946
				C(6)H	7.052
				C(7)H	7.310
				N(1)H	10.211
I16	8.674	3.523	2.154	γCH_2	2.126
					1.183
				γCH_3	0.914
				δCH_3	0.919
I17	8.522	3.551	1.958	γCH_2	1.812
					1.161
				γCH_3	0.908
				δCH_3	0.807
D18	8.747	4.365	2.990		
			2.659		
T19	8.062	3.697	4.073	γCH_3	0.981
V20	8.427	3.663	2.182	γCH_3 (*pro-S*)	0.948
				γCH_3 (*pro-R*)	1.037
N21	8.337	4.500	2.883		
			2.704		
K22	7.994	3.949	1.806		
			1.666		
F23	7.961	4.487	3.259	C(2,6)H	7.338
			3.057	C(3,5)H	7.209
				C(4)H	7.214
T24	7.759	4.280	4.252	γCH_3	1.284
K25	8.023	4.213	1.868		
K26	8.017	4.370	1.901		
			1.767		

three structures, together with the two starting structures obtained by model building, LDHL and HDHL (see Materials and Methods), were subjected to energy minimization and RMD as described under Materials and Methods.

The results of this structure refinement are shown in Table III, where the potential energies (E_{pot}) and the distance restraint energies (E_{res}) for the five calculated structures are listed. At equilibrium, the restraints energy, averaged over 10 ps, is non-zero but small and made up of several small deviations. This is attributable to the approximate evaluation of the input distances rather than to the trapping of the structure in local minima.

Table II: Comparison of φ Angles Deduced from $^3J_{NH-\alpha CH}$ Coupling Constants with Those from Averaging over the Last 10 ps of RMD for All Five Structures

	$^3J_{NH-\alpha CH}$[a]	ϕ_{exptl}[b]	ϕ_{av}
Met-1			
Ala-2	3.6	−55	−58
Gln-3	4.5	−63	−58
Asp-4	<6	−(45–72)	−60
Ile-5	<6	−(45–72)	−62
Ile-6	4.1	−59	−58
Ser-7	4.2	−60	−57
Thr-8	4.4	−62	−60
Ile-9	5.4	−70	−60
Gly-10			−57
Asp-11	4.2	−60	−59
Leu-12	<5	−(45–67)	−62
Val-13	<5	−(45–67)	−58
Lys-14	3.8	−56	−59
Trp-15	3.3	−52	−59
Ile-16	5.0	−67	−59
Ile-17	<5	−(45–67)	−59
Asp-18	2.9	−48	−60
Thr-19	5.4	−70	−68
Val-20	4.5	−63	−59
Asn-21	4.2	−60	−58
Lys-22	6.5	−78	−20
Phe-23	8.0	−149/−91	−71
Thr-24	7.7	−152/−88	−26
Lys-25	5.5	−70	−100
Lys-26	8.5	−144/−96	−85

[a] Mostly measured from 1D spectra with 0.3 Hz/point digital resolution. In cases where only limits are given, the values were estimated from DQF COSY spectra. [b] Experimental values of *J* can imply more than one value of φ; in the regions where the structure is known to be helical from NOE data, only those φ values nearest those of a standard helix are given.

Figure 3 shows the five structures obtained, superimposed to give the best fit between residues 3 and 22. All five final structures are reasonably consistent with the NMR data, although that from HDHL shows the lowest potential energy. Inspection of the five structures shows good agreement between them in the region from residues 2 to 20 (rms deviation = 0.039 nm) but a rather larger deviation over the whole molecule (rms deviation = 0.21 nm). This is not surprising since the terminal regions are less well-defined by the NMR data than the rest of the chain (see Figure 4), suggesting a higher flexibility.

A variety of different distance constraints can be applied in molecular dynamics. The usual constraints are from NOE data, but other possible restraints are donor–acceptor distances in hydrogen bonds and the intraresidue NH–αCH proton distances deduced from coupling constants and estimated dihedral angles. These additional restraints can be important in larger globular structures but they add relatively little information in δ-hemolysin. It is also worth noting that while proton NMR can identify slowly exchanging hydrogens, which may be the donor NH group in a hydrogen bond, the acceptor atom cannot be identified directly but only inferred.

In this study, coupling constants and amide hydrogen exchange data were not used in the determination of the structure but as an independent check on the consistency of the structure with experimental data. Table II shows a comparison between the φ angles deduced from experimentally determined *J* values and the average values for φ found in the calculated structures. It can be seen that there is a high level of agreement up to residue 21.

Table III: Potential and Restraints Energies of the Five δ-Hemolysin Structures at Different Stages of the Calculations[a]

	initial		after EM		after MD		after MD and EM	
	E_{pot}	E_{res}	E_{pot}	E_{res}	E_{pot}	E_{res}	E_{pot}	E_{res}
HDHL	$>10^5$	301	−598	269	−677	19	−1371	12
LDHL	$>10^5$	7409	6576	6085	−642	21	−1255	10
DIS1	$>10^5$	32	−585	89	−625	22	−1317	17
DIS2	$>10^5$	28	−553	62	−601	29	−1246	31
DIS3	$>10^5$	40	−443	74	−632	21	−1299	19

[a] The units are kilojoules per mole, but the zero is arbitrary.

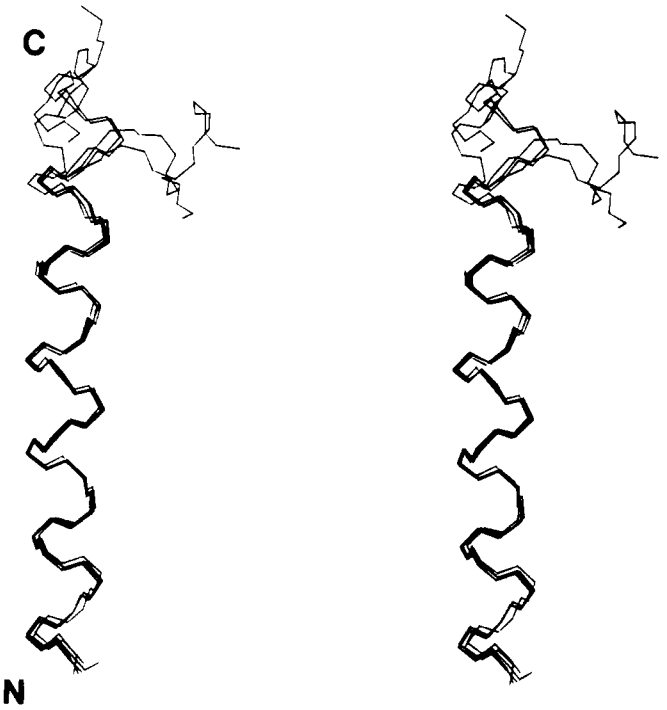

FIGURE 3: Stereoview of the structures obtained by averaging the final 10 ps of the restrained molecular dynamics runs. The best fit was calculated between residues 3 and 22. Only the backbones are shown, side chains being less well-defined. Charged residues occur on one face of the helix only, viz., Asp-4,11,18, Lys-14,22,25,26.

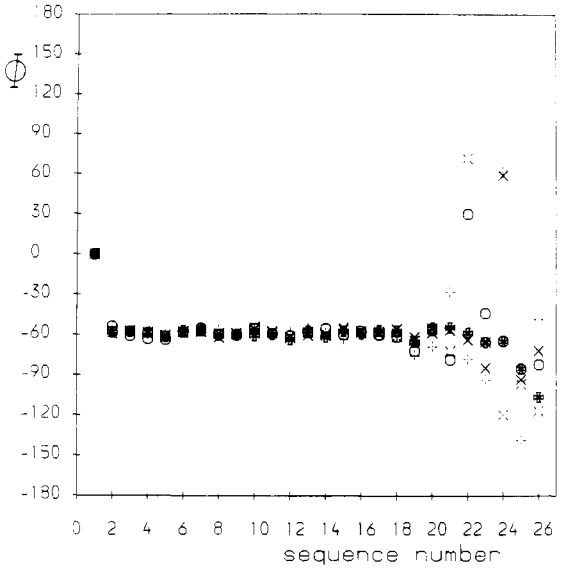

FIGURE 4: Comparison of the ϕ angles for each residue in the five structures LDHL, HDHL, DIS1, DIS2, and DIS3 averaged over the final 10 ps of restrained molecular dynamics. A different symbol is used for each of the five structures.

The slowly exchanging amide hydrogens, observed between residues 8 and 20, are also consistent with an ordered structure in this region. It should be noted that the first four amide hydrogens at the N-terminal end of an α-helix would be expected to exchange relatively quickly because of the absence of hydrogen bonds.

Discussion

It has been demonstrated here that δ-hemolysin forms a well-ordered helical structure, between residues 2 and 20, in methanol solution at low pH*. The C-terminal end appears to be relatively flexible. These conclusions, which were deduced purely from nuclear Overhauser effect data, were confirmed by independent analysis of spin-coupling constants and amide hydrogen exchange data. This approach presents a new way of assessing the validity of structure determinations from NMR data.

Although this structure has been determined in methanol, it is strikingly similar to a lower resolution structure obtained by NMR with the molecule bound to micelles (Lee et al., 1987). This has interesting implications for the study of transmembrane peptides using organic solvent systems, in that it appears that the structure of such peptides in a simple solvent such as methanol may mimic that in a more realistic but more complex environment.

It should be noted that while δ-hemolysin is relatively rigid in its central portion, two other transmembrane peptides, alamethicin and melittin, appear to contain a relatively flexible region near the center of the molecule (Fox & Richards, 1982; Vogel & Jahnig, 1986). While it is fairly clear that both alamethicin and melittin can form voltage-gated ion channels, the evidence for similar behavior by δ-hemolysin is less certain (Bernheimer & Rudy, 1986). These differences in flexibility could contribute to differences in function.

Another feature of the δ-hemolysin structure that has been noted before (Freer & Birkbeck, 1982; Lee et al., 1987) is the distribution of charge in the molecule. Charged residues occur at regular intervals in the sequence, corresponding to turns of a helix. Our study, indicating a helical structure, thus confirms the arrangement of charged residues along one face of the helix.

It seems likely that these charges will interact strongly with each other, especially in a medium of low dielectric constant. We note that Asp-11/Lys-14 and Asp-18/Lys-22 are likely candidates to form intramolecular salt bridge pairs. We are currently investigating the ionization states of all the ionizable groups by pH titration in methanol so as to define any electrostatic interactions in the molecule. While we have not determined the state of aggregation of the molecule in methanol, we believe it likely that a head to tail dimer is formed, allowing an interaction between Lys-25 and Asp-4.

Acknowledgments

This is a contribution from the Oxford Enzyme Group. We thank the Laboratory of Molecular Biophysics, Oxford, for the use of their graphics facilities. We also thank Prof. Wilfred

van Gunsteren and Dr. Werner Braun for the GROMOS and DISSMAN programs, respectively.

Registry No. δ-Hemolysin, 74838-20-3.

REFERENCES

Aqvist, J., van Gunsteren, W. F., Leijanmarck, M., & Tapia, O. (1985) *J. Mol. Biol. 183*, 461.

Bax, A., & Drobny, G. (1985) *J. Magn. Reson. 61*, 306.

Berendsen, H. J. C., Postma, J. P. M., van Gunsteren, W. F., & Hermans, J. (1981) in *Intermolecular Forces* (Pullman, B., Ed.) pp 331–342, D. Reidel, Dordrecht, The Netherlands.

Bernheimer, A. W., & Rudy, B. (1986) *Biochim. Biophys. Acta 864*, 123.

Bhakoo, M., Birkbeck, H., & Freer, J. H. (1982) *Biochemistry 21*, 6879.

Bodenhausen, G., Vold, R. L., & Vold, R. R. (1980) *J. Magn. Reson. 37*, 93.

Braun, W., & Go, N. (1985) *J. Mol. Biol. 186*, 611.

Braun, W., Wagner, G., Wörgötter, E., Vasak, M., Kagi, J. H. R., & Wüthrich, K. (1986) *J. Mol. Biol. 187*, 125.

Clore, G. M., Nilges, M., Brunger, A. T., Karplus, M., & Gronenborn, A. M. (1987) *FEBS Lett. 213*, 269.

Eich, G. W., Bodenhausen, G., & Ernst, R. R. (1982) *J. Am. Chem. Soc. 104*, 3731.

Eisenberg, D. (1984) *Annu. Rev. Biochem. 53*, 595.

Fox, R. O., & Richards, F. M. (1982) *Nature (London) 300*, 325.

Freer, J. H., & Birkbeck, T. H. (1982) *J. Theor. Biol. 94*, 535.

Hoult, D. I., & Richards, R. E. (1975) *Proc. R. Soc. London, A 344*, 311.

Jeener, J., Meier, B. H., Bachmann, P., & Ernst, R. R. (1979) *J. Chem. Phys. 71*, 4546.

Kumar, A., Ernst, R. R., & Wüthrich, K. (1980) *Biochem. Biophys. Res. Commun. 95*, 1.

Kuntz, I. D., Crippen, G. M., Kollman, P. A., & Kimelman, D. (1976) *J. Mol. Biol. 106*, 983.

Lee, K. H., Fitton, J. E., & Wüthrich, K. (1987) *Biochim. Biophys. Acta 911*, 144.

Macura, S., Huang, Y., Suter, D., & Ernst, R. R. (1981) *J. Magn. Reson. 43*, 259.

McCammon, J. A., Gelin, B. R., & Karplus, M. (1977) *Nature (London) 267*, 585.

Pardi, A., Billeter, M., & Wüthrich, K. (1984) *J. Mol. Biol. 180*, 741.

Piantini, U., Sørensen, O. W., & Ernst, R. R. (1982) *J. Am. Chem. Soc. 104*, 6800.

Rance, M., Sørensen, O. W., Bodenhausen, G., Wagner, G., Ernst, R. R., & Wüthrich, K. (1983) *Biochem. Biophys. Res. Commun. 117*, 479.

Ryckaert, J. P., Ciccotti, G., & Berendsen, H. J. C. (1977) *J. Comput. Phys. 23*, 327.

Thomas, D. H., Rice, D. W., & Fitton, J. E. (1986) *J. Mol. Biol. 192*, 675.

Tosteson, M. T., & Tosteson, D. C. (1981) *Biophys. J. 36*, 109.

van Gunsteren, W. F., & Berendsen, H. J. C. (1977) *Mol. Phys. 34*, 1311.

van Gunsteren, W. F., Kaptein, R., & Zuiderweg, E. R. P. (1983) in *Nucleic Acid Conformation and Dynamics* (Olson, W. K., Ed.) pp 79–92, Report of NATO/CECAM Workshop, Orsay, France.

Vogel, H., & Jähnig, F. (1986) *Biophys. J. 50*, 573.

Wüthrich, K., Wider, G., Wagner, G., & Braun, W. (1982) *J. Mol. Biol. 155*, 311.

Wüthrich, K., Billeter, M., & Braun, W. (1984) *J. Mol. Biol. 180*, 715.

Yianni, Y. P., Fitton, J. E., & Morgan, C. G. (1986) *Biochim. Biophys. Acta 856*, 91.

Zuiderweg, E. R. P., Boelens, R., & Kaptein, R. (1984) *Biopolymers 24*, 601.